J. Trop. Resour. Sustain. Sci. 6 (2018): 50-56

Journal of Tropical Resources and Sustainable Science

journal homepage: jtrss.org

Bandgap tunability from synergistic mixture of *Pandanus amaryllifolius* and *Curcuma longa* as photo-absorber candidates

Nik Muhammad Muqit Ali[1], Khairul Nizar Syazwan W.S.W.[1], Syed Muhammad Al-Amsyar[2], Hasiah Salleh[3], Hasyiya Karimah Adli[1,*]

[1]Faculty of Bioengineering and Technology, Universiti Malaysia Kelantan, Kelantan, Malaysia
[2]Faculty of Agro Based Industry, Universiti Malaysia Kelantan, Kelantan, Malaysia
[3]Centre for Fundamental and Liberal Education, Universiti Malaysia Terengganu, 21030 Kuala Terengganu, Terengganu, Malaysia

Received 11 November 2017
Accepted 23 April 2018
Online 26 June 2018

Keywords:
electronic bandgap; hybrid; natural dyes extracts; sensitizer

⌧*Corresponding author:
Dr. Hasyiya Karimah Adli,
Faculty of Bioengineering and Technology,
Universiti Malaysia Kelantan,
Malaysia.
Email: hasyiya@umk.edu.my

Abstract

The application of natural plant-derived dyes to replace ruthenium-based material as photo-absorber in solar cells application, have been extensively studied. Several advantages such as low cost, abundant in supply, sustainability and environmentally-safe make natural materials as current favourite photo-absorber. Natural plant-derived dyes are known containing natural compounds (e.g. carotenoids, chlorophylls, anthocyanins) that have the characteristics of electronic delocalization in extended π-orbital system involving in electronic transfer mechanism. To date, massive investigations were done to exploit this system to be used as a potential photo-absorber in solar cells. Due to this matter, the hybrid dyes from the mixture of *Pandanus amaryllifolius* (pandan, **P**) and *Curcuma longa* (turmeric, **T**) were successfully prepared and several physical characterizations were carried out to analyse the photo-absorber (sensitizer) properties. From the results obtained, the ratios of **P**:**T** was varied into 1:2, 1:4, 4:1, and 8:1. This ratio has changed the wavelength of absorbers that were slightly shifted and the indirect bandgap (Eg) also were significantly changed. With this new approach, the bandgap of the hybrid dyes as core point in modulating electrical conductivity of photo-absorber can be simply tuned. By implying two different extract dyes to form hybrid dyes, the bandgap was found decreased with higher ratio of **T** used. Overall results suggesting that by adjusting the ratio of hybrid dyes, the photo-absorber properties and the Eg values were differed and with slightly modification, better electrical conductivity can be expected for solar cells application.

1. INTRODUCTION

The industrial revolution leads to overconsumption of non-renewable energy resources which take hundreds or thousands of years to replenish (Caineng *et al.*, 2016). The acute consumption also has led to the energy depletion and associated environmental issues. The renewable energy such as solar, geothermal, wind and biomass energy act as alternative resources and running in various countries to reduce dependence on traditional fossil fuels.

The unlimited sunlight source is feasible and worthy to be harvested as energy from sunlight strikes earth in one hour is greater than energy consumes in a year (Lewis, 2007). To harvest energy from the sunlight, solar cell is used to convert light (photon) into electricity by photovoltaic effect. The discovery of photoelectrochemical effect in 1839 has intrigued mass study in photovoltaic technology (Sauvage, 2014; Hug *et al.*, 2014). Following the exploration, dye sensitized solar cells (DSSC) concept was introduced in 1991 by imitating the photosynthesis process (Prima *et al*., 2017). DSSC has a number of attractive features, such as low cost, ease of fabrication and environmental friendly (Sawhney & Satapathi, 2017). A DSSC model structure is sandwich-like arrangement with photo-absorber/photo-sensitizer (dye pigment) as an essential layer that absorb photons light which has similar function of chlorophyll in leaves, together with porous layer of photoanode (e.g. titanium dioxide; TiO_2), a cathode (a metal counter electrode) and an electrolyte for dye regeneration (Will, 2013). Few factors need to be considered to ensure high solar performance of DSSC, including the choice of photo-sensitizer dye used (Abdel-Latif *et al.*, 2016). It is necessary to further improve the solar cell performance and in the same time, to reduce the cost of DSSCs for successful commercialization. It has been reported that the application of few dyes with complementary absorption spectra would broaden the spectral sensitivity of the cell, resulting in higher photo-conversion efficiency

(Bandara & Weerasinghe, 2006). Much efforts have been carried out, including tandem DSSCs (Murayama *et al.*, 2008), hybrid DSSCs (Noma *et al.*, 2009), and co-sensitized DSSCs based on TiO_2 (Choi *et al.*, 2008), which proven can improve the efficiencies of DSSCs to a certain extent.

To date, numerous studies reported on the design engineering and photo-sensitizer performance to increase its function efficiency (Mathew *et al.*, 2014). Natural dyes extracted from fruits, leaves, and vegetables are extensively reported with various solar cell performances (Iswariya *et al.*, 2017; Al-Alwani *et al.*, 2017; Calogero *et al.*, 2015; Hug *et al.*, 2014). Common natural dyes contain important pigments for photosynthesis, namely anthocyanin, chlorophyll etc. are easier for preparation, cheaper, eco-friendly and biodegradable, replacing traditional synthetic dyes (e.g.ruthenium, phorphyrin) (Yüzbaşıoğlu *et al.*, 2017; Gong *et al.*, 2017). The disadvantage of using a single natural dye is that the dye works in a narrow range of solar spectrum, which would minimize the cell efficiency. To characterize the electronic properties of materials, the optical absorption measurements are widely used through the determination of parameters describing the electronic transitions such as bandgap, valence band tails and excited state lifetime (Laidani *et al.*, 2008). The measurement of the bandgap of materials is considered as starting point to evaluate the potential of specific material could absorb a portion of solar spectrum. The term "bandgap" (Eg) refers to the energy difference between the top of the valence band to the bottom of the conduction band (as shown in Figure 1). In order for an electron to jump from valence band to conduction band, it requires a specific minimum amount of energy for the transition (Soto-rojo *et al.*, 2016).

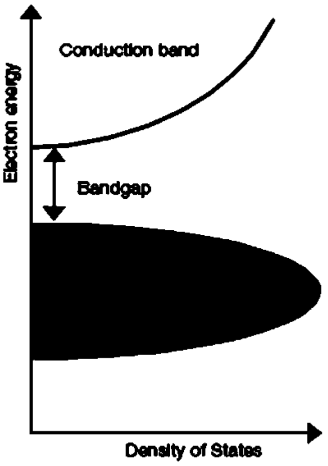

Figure 1: Minimum energy required for electron transfer, or also known as bandgap energy (Moia *et al.*, 2015)

Previous literature commonly focused on different natural dyes, types and compositions that influence on the solar performance (Kushwaha *et al.*, 2013). Whilst, it is widely known that the increase in band gap of a semiconductor has drastic changes in electrical and optical properties, in which bandgap is a critical parameter from application point of view. To achieve the objectives of the study, the hybrid dyes from *Pandanus amaryllifolius* (pandan, **P**) and *Curcuma longa* (turmeric, **T**) in different ratios were prepared to analyse their photo-absorption properties from spectral characterization and to evaluate the resulted bandgap values.

2. MATERIALS AND METHODS

2.1. Preparation of natural dyes extracts and hybrid dye solutions

The preparation of natural dyes extracts was done based on the literature with some modifications (Okoli *et al.*, 2012). About 30 g of fresh *Pandanus amaryllifolius* (pandan, **P**) leaves were washed with distilled water, blended in 70 % ethanol and properly was stored under dark condition for overnight. In the same manner, solution of *Curcuma longa* (turmeric, **T**) was stored under dark condition for overnight after dissolving in ethanol. Both solutions were then filtered with 0.45 µm Whatman filter paper to remove solid residues and centrifuged to finally obtain the natural dyes extracts.

The hybrid dye solution containing both dyes were prepared in different ratios; 1:2, 1:4, 4:1, and 8:1, denoted as X**P**: Y**T** (X, Y = number; **P** = Pandan; **T**= Turmeric), e.g., when 1 mL pandan solution was added with 2 mL Turmeric is denoted as 1**P**: 2**T**. The natural dye extracts and the hybrid dye solutions were properly stored and protected from direct sunlight, for further characterization.

2.2. Characterization

The absorption spectra of natural dyes extracts; *Pandanus amaryllifolius* (pandan, **P**) and *Curcuma longa* (turmeric, **T**) and hybrid dye solutions of 1**P**:2**T**, 1**P**:4**T**, 4**P**:1**T** and 8**P**:1**T** were determined using UV-Vis spectrophotometer (Spectrophotometer HACH DR 5000) in the wavelength range of 400–800 nm. From the absorption spectra, the bandgap of each dyes and mixture solutions were calculated by using Tauc method. The spectral properties of natural dye extracts and hybrid dye solutions were studied using Fourier Transform Infrared (FTIR) spectroscopy, recorded from 400 cm^{-1} until 4000 cm^{-1} (Perkin Elmer Spectrum™ 400 FTIR-ATR Spectrometer). GC-MS analysis also was carried out using Perker-Elmer Clarus 680 system coupled with Clarus 600 (EI) Mass spectrometer (MS). For GC-MS detection, the ethanol was used as solven and an electron ionization system was operated in electron impact mode with ionization energy of 70 eV. Helium gas (99.999 %) was used as carrier gas at a constant flow rate of 1 ml/min and an injection volume of 2 µl was employed (split ratio of 10:1). The injector temperature was maintained at 250°C, the ion-source temperature at 200°C, and the oven temperature was programmed at 110°C (isothermal for 2 min), with an increase of 10°C/min to 200°C, then

5°C/min to 280°C, ending with 9 min isothermal at 280°C. Mass spectra were taken at 70 eV with a scan interval of 0.5 seconds and fragments from 45-450 Da. The delay time was set from 0 to 2 min and the total GC-MS running time was 36 min.

3. RESULTS AND DISCUSSION

The prepared hybrid dye exhibit homogeneous solution with the changes of color after mixing both dyes extracts (**P** and **T**). Figure 2 shows the photos of dyes extracts from *Pandanus amaryllifolius* (pandan, **P**), *Curcuma longa* (turmeric, **T**) and hybrid dye solutions of 1**P**:2**T**, 1**P**:4**T**, 4**P**:1**T** and 8**P**:1**T**.

The absorption analysis of all prepared solutions was determined from UV-Vis spectroscopy, as shown in Figure 3.. The absorption spectra of all dyes extracts showed the presence of distinct absorption peaks in the visible region from 300 until 800 nm. *Pandanus amaryllifolius* (pandan, **P**) extract dye presents strong absorption bands at about 415 nm and 660 nm, showing characteristic of chlorophyll green pigment (Porrarud & Pranee, 2010; Al-Alwani *et al.*, 2014). Generally, chlorophyll exhibits an absorption band in the intense range of visible light due to charge-transfer transition from the highest occupied molecular orbital (HOMO) in the ground state to the lowest unoccupied molecular orbital (LUMO) in the excited state. This makes chlorophyll as suitable material as photo-absorber in the visible-light region (Kuo *et al.*, 2011). Meanwhile, the absorption peak of *Curcuma longa* (turmeric, **T**) can be seen at wavelength range between 400 to 550 nm. It is known that curcumin is a naturally occurring chemical compound could be derived from **T** has a long intense wavelength absorption range from 420 - 580 nm in the visible region (Syafinar *et al.*, 2015). These broad UV absorption spectrums is related to the presence of phenolic groups in curcumin and the electron excitation from the π→π* transition which is highly polar due to intramolecular charge transfer from the phenyl ring towards the carbonyl moiety (Zsila *et al.*, 2003). By mixing **P** and **T** extracts dyes, UV absorption spectra in Figure 3.0 display the successful mixture of **P** and **T**, with the existence of both main peaks located in the whole visible region. With the ratio of 1 **P**: 4 **T**, the main peak of chlorophyll was observed around 660 nm, and higher ratio of **P** mixed with **T** extracts (e.g. 4 **P**: 1 **T**), the distinct absorption peak of chlorophyll was found gradually increased. Besides, the significant blue-shifted of slope to the shorter wavelength was noticed when the ratio of **P** increased, might be due to the changes of structural properties occur due the mixing of dyes extract. Overall, the obtained UV-vis spectra indicated that by mixing different dyes extracts which have different absorption band in visible region could effect on the changes of photo-absorption properties.

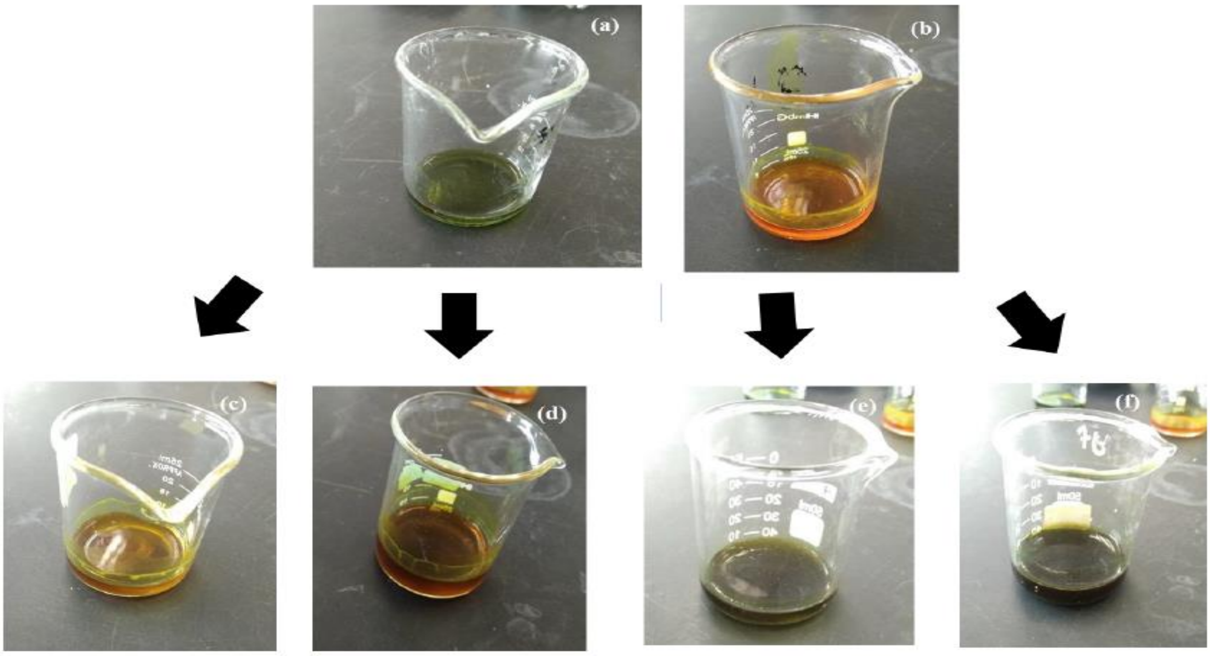

Figure 2: Pictures of (a) **P**, (b) **T**, (c) 1 **P**: 2 **T**, (d) 1 **P**: 4 **T**, (e) 4 **P**: 1 **T**, and (f) 8 **P**: 1 **T**, respectively

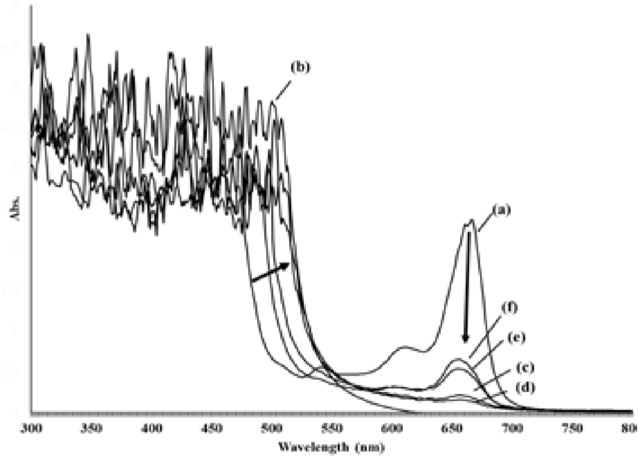

Figure 3: UV absorption spectra of (a) **P**, (b) **T**, (c) 1 **P**: 2 **T**, (d) 1 **P**: 4 **T**, (e) 4 **P**: 1 **T**, and (f) 8 **P**: 1 **T**, respectively

Table 1: Tauc model (bandgap calculation)

Band Gap Energy (E) = hc/λ				
Planck constant (h) = 6.63 x 10^{-34} Joules sec (J.s)				
Speed of light (C) = 3.00 x 10^{8} meter/sec (m/s)				
Cut off wavelength (λ) = *obtained from UV-vis absorbance spectrum in meters				
h	**C**	**λ**	**E**	**eV**
6.63×10^{-34}	3.00×10^{8}	4.11×10^{-7}	4.84×10^{-19}	3.03
Where 1 eV = 1.6 x 10^{-19} Joules (conversion factor)				

The Tauc model is known as the standard empirical model whereby the optical gap of an amorphous semiconductor and amorphous phthalocyanines films may be determined. Based on the Tauc model, the optical bandgap was calculated using absorption edge values (λ edge, in nm) from absorption spectra using following equation summarized in Table 1. The Tauc optical gap is determined through an extrapolation of the linear trend observed in the spectral dependence of $(\alpha h\nu)^{1/2}$ over a limited range of photon energies hν (Mok *et al.,* 2007). Figure 4 shows the Tauc plot derived from UV-vis-spectrum of dyes extracts and hybrid dyes respectively. The estimation of the optical bandgap was made based on the intersection of the dashed line with the x-axis. It can be clearly shown that the changes of bandgap values in relation to the ratio of respective hybrid dyes. As summarized in the table (inset), **P** recorded the largest bandgap value of 2.54 eV and the value was found decreased to 0.22 eV when **P** extract dyes was mixed with 2 parts of **T**. The synergistic mixture of both extract dyes also contributed to the shifter wavelength to the higher wavelength (from Figure 3) and thus decreased the bandgap value. From the ratio of 1**P**: 4**T**, it is noticeable that the Eg value was reduced from 2.54 eV of **P** or 2.35 of **T** to 2.30 eV. This analysis concluded that by simply tuning the ratio of hybrid dyes, the changes of Eg value could be expected. From the series of dyes extracts, the 1**P**: 4**T** dyes solution recorded shortest Eg values, which can be determined due to the composition an improvement of the photoelectric conversion efficiency (Del Caño *et al.,* 2005).

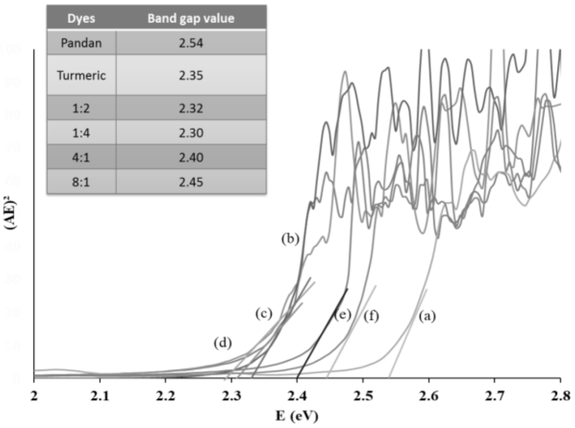

Dyes	Band gap value
Pandan	2.54
Turmeric	2.35
1:2	2.32
1:4	2.30
4:1	2.40
8:1	2.45

Figure 4: Tauc plot derived from UV-vis-spectrum of (a) **P**, (b) **T**, (c) 1**P**: 2**T**, (d) 1**P**: 4**T**, (e) 4**P**: 1**T**, and (f) 8**P**: 1**T**, respectively

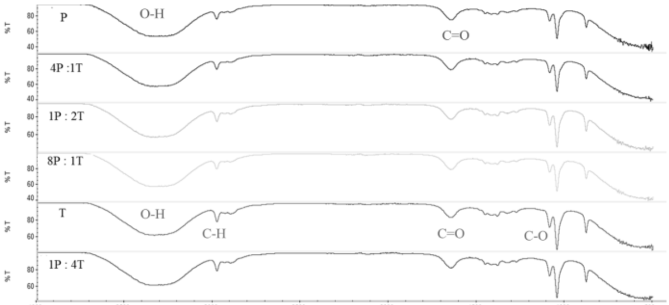

Figure 5: FTIR spectra of dyes extracts and hybrid dyes solutions

The FT-IR analysis also was carried out to identify the most important and representative bonds of dyes extracts. Figure 5 shows FTIR spectra of all dyes extracts and hybrid dye solutions with characteristic bands of **P** and **T** recorded in the region of 4000 – 400 cm^{-1}. There is no additional new peak observed from hybrid dyes spectra, verify that the mixing approach is might form physical interaction between **P** and **T**. The notable peaks of the extract dyes can be found at 3300, 3000, 1700 and 1200 cm^{-1} resulted from O-H, CH-H, C=O and C-O, respectively (Pawar *et al.*, 2014; Faiz & Fahmi, 2016).

The presence of the main active inredients in *Pandanus amaryllifolius* (pandan, **P**) and *Curcma longa* (turmeric, **T**) were corroborated by using Gas Chromatography-Mass Spectrometry (GC-MS). The main components present in **P** including stigmasterol (r.t. 26.171), phytol (r.t. 17.278), ethyl iso-allocholate (r.t. 10.019), and 2-ethylcyclohexyl ester m-toluic acid (r.t. 4.701), respectively. Phytol and m-Toluic acid are widely known as one of the determinants of chlorophyll interactions in solution and aromatic compound in *Pandanus amaryllifolius* (Fiedor *et al.,* 2003; Wakte *et al.,* 2012). Whilst, four major compounds were identified from *Curcuma longa* (turmeric, **T**) which are 1-2-hydroxyl-5-methylphenyl (r.t. 5.904), ar-tumerone (r.t. 10.206), 1-heptatriacotanol (r.t. 14.704), and 6-octadecenoic acid (r.t. 16.941), as shown in Table 2.0.

Ar-tumerone was traced in all extract dye solution except in **P**. Main components of **P** and **T** were figured out from all hybrid dyes solution (Negi *et al.*, 1999), confirming that the interactions of both dyes in the solution. Figure 6 and 7 display GC-mass spectra of **P** and **T** extraction. Table 2 shows the list of main components detected from the dyes extracts; *Pandanus amaryllifolius* (pandan, **P**) and *Curcuma longa* (turmeric, **T**).

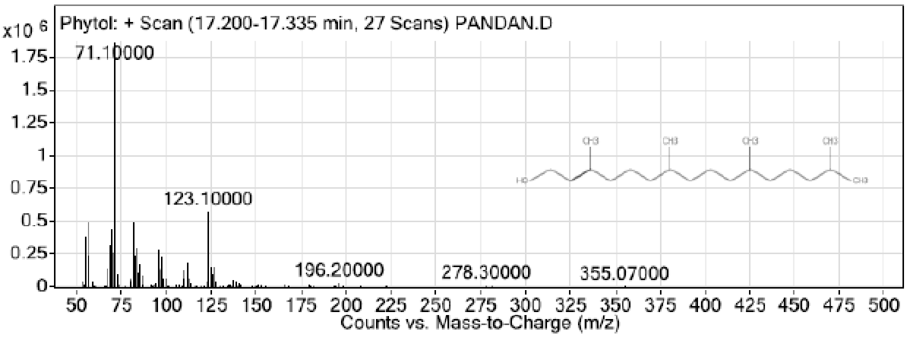

Figure 6: GC-Mass spectrum of phytol in *Pandanus amaryllifolius sp.* (pandan, **P)** extraction

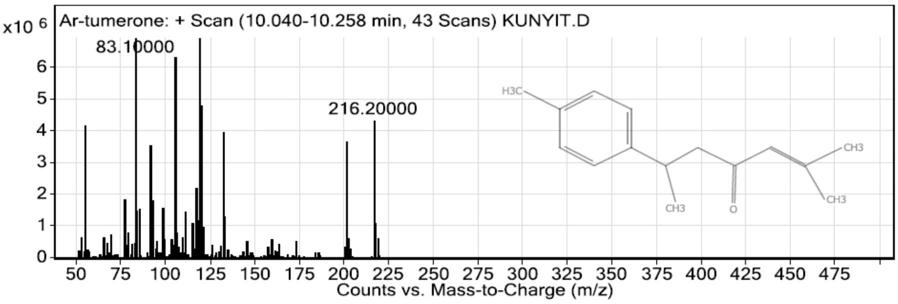

Figure 7: GC-Mass spectrum of turmerone in *Curcuma longa sp.* (turmeric, **T**) extraction

Table 2: Identified components present

Extract Dyes/ Hybrid Dyes in ethanol	Retention time, rt (minute)	Name	Molecular weight (g/mol)
***Pandanus amaryllifolius sp.* (Pandan, P)**	4.701	2-ethylcyclohexyl ester m-toluic acid	246.35
	10.019	Ethyl iso-allocholate	436.63
	17.278	Phytol	296.54
	26.171	stigmasterol	412.7
***Curcuma longa sp.* (Turmeric, T)**	5.904	1-2-hydroxyl-5-methylphenyl	150.175
	10.206	Ar-tumerone	216.324
	14.704	1-heptatriacotanol	537.014
	16.941	6-Octadecenoic acid	282.468
1P:4T	5.904	1-(2-hydroxy-5-methylphenyl)-ethanone	150.177
	10.174	Ar-tumerone	216.324
	14.626	1-heptatriacotanol	537.014
	17.247	1-Heptatriacotanol	537.014
4P:1T	4.685	2-ethylcyclohexyl ester m-Toluic acid	246.35
	7.912	1-(1,5-dimethyl-4-hexenyl)-4-methyl-Benzene	202.3352
	10.112	Ar-tumerone	216.324
	14.554	2-Butenoic acid, 2-methyl-, 2-(acetyloxy)1,1a,2,3,4,6,7,10,11,11a-decahydro-7,10-dihydroxy 1,1,3,6,9-pentamethyl-4a,7a-epoxy	532.63
8P:1T	4.695	2-ethylcyclohexyl ester m-Toluic acid	246.35
	7.917	1-(1,5-dimethyl-4-hexenyl)-4-methyl-Benzene	202.3352
	10.102	Ar-tumerone	216.324
	14.538	2-methyl-, 2-(acetyloxy)-1,1a,2,3,4,6,7,10,11,11a-decahydro-7,10-dihydroxy-1,1,3,6,9-pentamethyl-4a,7a-epoxy 2-Butenoic acid	532.63
	17.262	Phytol	296.54

4. CONCLUSION

The dyes extract of *Pandanus amaryllifolius* (pandan, **P**) and *Curcuma longa* (turmeric, **T**) and the hybrid dyes of 1**P**: 2**T**, 1**P**: 4**T**, 4**P**: 1**T** and 8**P**: 1**T** were successfully extracted and prepared. The extract dyes solutions were characterized by Ultraviolet-Visible Spectroscopy (UV-Vis), Fourier Transform Infrared (FTIR) and Gas chromatography–mass spectrometry (GC-MS). The bandgap values of dyes extract, and hybrid dyes solution of **P** and **T** calculated from Tauc plot shows the smallest bandgap was obtained from high ratio of **T**. With the hybrid dyes solution (X**P**:Y**T**), the bandgap can be further decreased from 2.54 eV (**P**) / 2.35 eV (**T**) to 2.30 eV (1**P**:4**T**). Thus, by simply tuning the ratio of different extract dyes, the changes of photo-absorption in visible wavelength and the bandgap values can be expected. The results obtained suggest that the potential of *Pandanus amaryllifolius sp.* and *Curcuma longa sp.* hybrid dyes solution as photo-absorber in solar cells. With further optimization on the spectral study and the ratio of dyes, the application of these natural plant-extracted dyes in solar cells is still in progress.

ACKNOWLEDGEMENT

This research was financially supported by Short Term Research Grant (SGJP) (Grant No. R/SGJP/A13.00/00871A/001/2018/000456). Authors also pleased to acknowledge Principal & Liberal Education Center, Universiti Malaysia Terengganu for providing materials for the research. A million thanks also to lecturers and lab assistants of Universiti Malaysia Kelantan who indirectly involved in completing this study.

REFERENCES

Abdel-Latif, M. S., Batniji, A., El-Agez, T. M., Younis, M. J., Ghamri, H., Thaher, B. A. A., Qeshta, B. S., Abu-Awwad, F. M., Taya, S. A. (2016). Dye sensitized solar cells based on hydrazonoyl synthetic dyes. Journal of Nano- and Electronic Physics 8 (4(1)), 04038 – 04047.

Al-Alwani, A. M., Mohamad, A. B., Kadhum, A. A. H., Ludin, N. A., Safie, N. E., Razali, M. Z., Ismail, M., Sopian, K. (2017). Natural dye extracted from *Pandannus amaryllifolius* leaves as sensitizer in fabrication of dye-sensitized solar cells. Int. J. Electrochem. Sci., 747 – 761.

Al-Alwani, M.A.M., Mohamad, A.B., Kadhum, A.A.H., Ludin, N.A., Ba-Abbad, M.M. (2014). Effect of solvents on natural dyes adsorption on the surface of TiO_2 film for dye- sensitized solar cell. Australian Journal of Basic and Applied Sciences, 8(19), 34-37.

Bandara, J. Weerasinghe, H. (2006). Design of high-efficiency solid-state dye sensitized solar cells using coupled dye mixtures. Solar Energy Materials & Solar Cells, 90: 864–871.

Calogero, G., Bartolotta, A., Di Marco, G., Di Carlo, A., Bonaccorso, F. (2015). Vegetable-based dye-sensitized solar cells. **Chem. Soc. Rev.**, **44**, 3244-3294.

Choi H, Kim S, Kang S O, Ko J J, Kang M S, Clifford J, Forneli A, Palomares E, Nazeeruddin M K, Grätzel M. (2008). Stepwise cosensitization of nanocrystalline TiO_2 films utilizing Al_2O_3 layers in dye-sensitized solar cells. Angewandte Chemie International Edition, 47(43): 8259–8263.

Del Caño, T., Parra, V., Rodríguez Méndez, M.L., Aroca, R.F., de Saja, J.A. (2005). Characterization of evaporated trivalent and tetravalent phthalocyanines thin films: Different degree of organization. Appl. Surf. Sci. 246, 327–333.

Faiz, M. R., Fahmi, A. (2016). Performance of pandan leaf pigment for dye sensitized solar cell (dssc): effect of dye extraction temperature, JAVA. International Journal of Electrical and Electronics Engineering, 14, 1.

Fiedor, L., Stasiek, M., Myśliwa-Kurdziel, B., Strzałka, K. (2003). Phytol as one of the determinants of chlorophyll interactions in solution. Photosynthesis Research, 78 (1), 47–57.

Kushwaha, R., Srivastava, P., Bahadur, L. (2013). Natural Pigments from Plants Used as Sensitizers for TiO_2 Based Dye-Sensitized Solar Cells. Journal of Energy, 654953, 1-8.

Gong, J., Sumathy, K., Qiao, Q., Zhou, Z. (2017). Review on dye-sensitized solar cells (DSSCs): Advanced techniques and research trends. Renewable and Sustainable Energy Reviews, 68, 234–246.

Hug, H., Bader, M., Mair, P., Glatzel, T. (2014). Biophotovoltaics: Natural pigments in dye-sensitized solar cells. Applied Energy, 115, 216–225.

Iswariya, S., Dhanemozhi, M. A. C. Yugamica, S. (2017). Synthesis and characterization of dye sensitized solar cell using fruit extracts. International Research Journal of Engineering and Technology (IRJET), 04 (02), 277 – 285.

Laidani, N., Bartali, R., Gottardi, G., Anderle, M., Cheyssac, P. (2008). Optical absorption parameters of amorphous carbon films from forouhi-bloomer and tauc-lorentz models: A comparative study. *J. Phys. Condens. Matter. 20* (1), 015216.

Lewis, N. S. (2007). Toward cost-effective solar energy use. Science, 315, 798-801.

Sauvage, F. (2014). A review on current status of stability and knowledge on liquid electrolyte-based dye-sensitized solar cells. Advances in Chemistry, 1–23.

Mathew, S., Yella, A., Gao, P., Humphry-Baker, R., Curchod, B. F. E., Ashari-Astani, N., Tavernelli, I., Rothlisberger, U., Rothlisberger, M. K., Grätzel, M. (2014). Dye-sensitized solar cells with 13% efficiency achieved through the molecular engineering of porphyrin sensitizers. Nature Chemistry 6, 242–247.

Moia, D., Leijtens, T., Noel, N., Snaith, H. J., Nelson, J., & Barnes, P. R. F. (2015). Dye Monolayers Used as the Hole Transporting Medium in Dye-Sensitized Solar Cells. Advanced Materials, 27(39), 5889–5894.

Mok, T.M., O'Leary, S.K. (2007). The dependence of the Tauc and Cody optical gaps associated with hydrogenated amorphous silicon on the film thickness: αl Experimental limitations and the impact of curvature in the Tauc and Cody plots. J. Appl. Phys., 102, 113525:1–113525:9.

Murayama M., Mori T. (2008). Novel tandem cell structure of dye-sensitized solar cell for improvement in photocurrent. Thin Solid Films, 516(9): 2716–2722.

Negi, P. S., Jayaprakasha, G. K., Jagan Mohan Rao, L., & Sakariah, K. K. (1999). Antibacterial activity of turmeric oil: a byproduct from curcumin manufacture. Journal of agricultural and food chemistry, 47(10), 4297-4300.

Noma Y, Lizuka K, Ogomi Y, Pandey S S, Hayase S. (2009). Preparation of double dye-layer structure of dye-sensitized solar cells from cocktail solutions for harvesting light in wide range of wavelengths. Japanese Journal of Applied Physics, 48(2): 020213 – 020215.

Okoli L. U., Ozuomba J. O, Ekpunobi A. J. (2013). Influence of local dye on the optical band-gap of titanium dioxide and its performance as a DSSC material. Research Journal of Physical Sciences, 1(10), 6-10.

Pawar, H., Karde, M., Mundle, N., Jadhav, P., Mehra, K. (2014). Phytochemical evaluation and curcumin content determination of turmeric rhizomes collected from Bhandara District of Maharashtra (India), Med Chem, 4(8), 588-591.

Prima, E. C., Hidayat, N. N., Yuliarto, B., Suyatman, Dipojono, H. K. (2017). A combined spectroscopic and TDDFT study of natural dyes extracted from fruit peels of Citrus reticulata and Musa acuminata for dye-sensitized solar cells. Spectrochimica acta - part A: Molecular and Biomolecular Spectroscopy, 171, 112–125.

Porrarud, S., Pranee, A. (2010). Microencapsulation of Zn-Chlorophyll pigment from pandan leaf by spray dring and its characteristics. International Food Research Journal, 17, 1031-1042.

Sawhney, N., Satapathi, S. (2017). Utilization of naturally occurring dyes as sensitizers in dye sensitized solar cells, IEEE Journal of Photovoltaics 7 (21–11), 539 – 544.

Soto-rojo, R., Baldenebro-lópez, J., & Glossman-mitnik, D. (2016). Theoretical Study of the Bridge Influence with Different Units of Thiophene and Thiazole in Coumarin Dye-Sensitized Solar Cells. International Journal of Photoenergy, (2016), 1-8.

Syafinar, V., Gomesh, N., Irwanto, M., Fareq, M., Irwan, Y. M. (2015). Chlorophyll pigments as nature-based dye for Dye-Sensitized Solar Cell (DSSC), 79, 896-902.

Yüzbaşıoğlu, Elif, Dalyan, Eda, Akpinar, Ilgin. (2017). Changes in photosynthetic pigments, anthocyanin content and antioxidant enzyme activities of maize (Zea Mays L.) seedlings under high temperature stress conditions. Trakya University Journal of Natural Sciences, 18 (2), E1 – E8.

Wakte, K. V., Zanan, R. L., Thengane, R. J., Jawali, N., & Nadaf, A. B. (2012). Identification of elite population of Pandanus amaryllifolius Roxb. for higher 2-acetyl-1-pyrroline and other volatile contents by HS-SPME/GC-FID from Peninsular India. Food Analytical Methods, 5(6), 1276-1288.

Will, S. (2013). What is a dye-sensitized solar cell. Azonano website. http://www.azonano.com/article.aspx?ArticleID=3175.

Zsila, F., Bikádi, Z., Simonyi, M. (2003). Probing the binding of the flavonoid, quercetin to human serum albumin by circular dichroism, electronic absorption spectroscopy and molecular modelling methods, Biochem Pharmacol., 65(3), 447-56

eISSN Number: 2462-2389